

## Growth of twin-free heteroepitaxial diamond on Ir/YSZ/Si(111)

M. Fischer,<sup>1</sup> R. Brescia,<sup>1</sup> S. Gsell,<sup>1</sup> M. Schreck,<sup>1,a)</sup> T. Brugger,<sup>2</sup> T. Greber,<sup>2</sup>  
J. Osterwalder,<sup>2</sup> and B. Stritzker<sup>1</sup><sup>1</sup>*Institut für Physik, Universität Augsburg, D-86135 Augsburg, Germany*<sup>2</sup>*Physik-Institut, Universität Zürich, CH-8057 Zürich, Switzerland*

(Received 5 August 2008; accepted 20 September 2008; published online 30 December 2008)

Heteroepitaxial nucleation and growth of twin-free diamond on Ir(111) is reported. The bias enhanced nucleation (BEN) technique was applied in a microwave plasma chemical vapor deposition setup to induce diamond nucleation on the new multilayer stack Ir/YSZ/Si(111). We demonstrate that the gathering of the diamond nuclei in so-called “domains,” a pattern formation process unique for diamond nucleation on iridium, is also present on Ir(111). The 1–2 nm thick carbon layer deposited by BEN does not show any crystalline diamond structures in electron diffraction and high resolution lattice imaging microscopy. In contrast, x-ray photoelectron diffraction (XPD) measurements yield C 1s diffractograms with clear threefold symmetry. The main features are comparable to measurements on diamond (111) single crystal surfaces. The weaker fine structure in the XPD patterns of the BEN layers is attributed to some disorder due to the harsh ion bombardment. However, this ion bombardment did not induce any measurable amount of twinning as deduced from the threefold symmetry. After 3 h diamond growth, the signal due to twins in the x-ray diffraction pole figures is still below the noise level of ~1%. Negligible twinning and the low mosaic spread of 0.96° (tilt) and 1.85° (twist) indicate that these films mark a breakthrough toward heteroepitaxial diamond films with (111) orientation. They provide interesting growth substrates, e.g., for phosphorous doped diamond or for the formation of heterojunction devices by deposition of wurtzite-type wide band gap semiconductor materials. © 2008 American Institute of Physics. [DOI: 10.1063/1.3019046]

### I. INTRODUCTION

Due to its unique potential for the future realization of wafer-scale single crystals, heteroepitaxial diamond formation by the bias enhanced nucleation (BEN) procedure on iridium surfaces has been intensively studied in the last two decades.<sup>1–3</sup> Nearly all experiments were restricted to Ir(001) since diamond growth by chemical vapor deposition (CVD) gives the minimum defect densities in {001} growth sectors. For the Ir(001) surface, heteroepitaxial diamond films with single crystal structure have been realized.<sup>4</sup> In addition, different multilayer structures have been developed to provide (001)-oriented iridium with high structural quality for the subsequent deposition of heteroepitaxial diamond. These comprise Ir/MgO(001),<sup>5</sup> Ir/SrTiO<sub>3</sub>(001),<sup>2,3</sup> Ir(001)/Al<sub>2</sub>O<sub>3</sub>(11 $\bar{2}$ 0),<sup>6</sup> Ir/SrTiO<sub>3</sub>/Si(001),<sup>7</sup> and Ir/yttria-stabilized zirconia(YSZ)/Si(001).<sup>8</sup>

Basic constraints for diamond growth with high crystal-line quality on {111} facets arise from the difficulties to suppress contact twins.<sup>9</sup> Nevertheless, there are several areas where (111)-oriented layers would be of high interest. For instance in *n*-type doping experiments with phosphorous, a strong growth sector dependence of the impurity incorporation was observed, which favored *n*-type growth on (111)-oriented substrates.<sup>10,11</sup> Furthermore, diamond(111) could provide an ideal growth surface for (0001)-oriented wurtzite-

type semiconductors to form heterojunction devices. Finally, BEN on Ir(001) has shown several peculiarities such as the nucleation under etching conditions and especially the gathering of the nuclei in well-defined areas (“domains”).<sup>12</sup> The latter phenomenon has not been observed on other materials. The comparison of BEN on different crystallographic facets of Ir may yield valuable hints to understand the nucleation process on iridium in general.

In the present work we studied heteroepitaxial diamond growth on Ir(111). In a first step, single crystal iridium films were deposited on Si(111) via YSZ buffer layers. These Ir/YSZ/Si(111) multilayer samples were then subject to a BEN treatment. The formed carbon layer was characterized by different surface science tools and by cross section high resolution transmission electron microscopy (HRTEM). Finally, thin diamond layers were grown and their texture was determined by x-ray diffraction (XRD) pole figure measurements. It was found that twin-free heteroepitaxial diamond nucleation and growth with up to now unmatched low mosaic spread can be achieved on the new substrate system Ir/YSZ/Si(111) that is available in 4 in. wafer size.

### II. EXPERIMENTAL

Epitaxial YSZ films on 4 in. Si(111) wafers were prepared by pulsed laser deposition using a KrF excimer laser (pulse duration: 25 ns, pulse energy: 850 mJ) and a cylindrical ablation target. For the fabrication of the target we used a mixture of Y<sub>2</sub>O<sub>3</sub> and ZrO<sub>2</sub> powder (21.4 mol % YO<sub>1.5</sub>), which was compressed at 1.5 kbar and then sintered for 25 h

<sup>a)</sup> Author to whom correspondence should be addressed. Electronic mail: matthias.schreck@physik.uni-augsburg.de. Tel.: +49-821-598-3401. FAX: +49-821-598-3425.

at 1500–1650 °C. Ablation was done at a substrate temperature of 750 °C. To reduce the native oxide of the Si(111) substrate, the first 500–1000 pulses were performed in high vacuum. For further growth the oxygen background pressure was increased to  $5 \times 10^{-4}$  mbar. The typical film thickness was between 20 and 40 nm.

In the next step, 150 nm thick iridium films were deposited on the oxide buffered silicon by e-beam evaporation at 650 °C. The first 20 nm were grown with a low deposition rate of 0.004 nm/s. For the rest of the film a rate of 0.02 nm/s was applied.

Diamond nucleation was performed in a microwave plasma chemical vapor deposition (MWPCVD) setup on samples of  $1 \times 1$  cm<sup>2</sup>. BEN was done for 45 min at a temperature of 700–800 °C, a gas pressure of 35 mbar, and 1200 W microwave power with 5%–10% CH<sub>4</sub> in H<sub>2</sub>. A negative bias voltage of 250–280 V was applied to the substrate. For the subsequent growth the conditions were changed to 800 °C, 40 mbar, 2000 W microwave power, and a gas mixture of 1% CH<sub>4</sub> in H<sub>2</sub>.

The surface was examined by a LEO DSM 982 Gemini scanning electron microscope (SEM). The annular in-lens (IL) detector of this instrument allows to identify the areas of successful diamond nucleation and to deduce the fraction of surface coverage by domains. Reflection high energy electron diffraction (RHEED) patterns were taken with a STAIB RHEED system operated at 30 kV in order to study the crystalline order of the nucleation layer. TEM micrographs were acquired using a JEOL field-emission microscope JEM-2100F operated at 200 kV. XRD  $\Theta$ – $2\Theta$  scans and measurements of the mosaic spread were done by a Seifert XRD 3003 PTS-HR. Pole figures were measured with a Siemens D5000 x-ray diffractometer. Both diffractometers work with Cu K $\alpha$  radiation. X-ray photoelectron diffraction (XPD) experiments were performed in a modified VG ESCALAB 220 photoemission spectrometer with a base pressure in the low  $10^{-10}$  mbar region using Mg K $\alpha$  radiation.<sup>13</sup>

### III. RESULTS

#### A. The multilayer stack Ir/YSZ/Si(111)

Epitaxial iridium deposition on silicon requires a crystalline oxide buffer.<sup>14</sup> As recently shown for deposition on Si(001), an YSZ buffer layer is a viable candidate.<sup>8</sup> The orientation of YSZ films on Si(001) is identical to that of the substrate. In the present experiments on Si(111), however, the oxide crystal lattice is azimuthally rotated by 60° relative to the silicon lattice.

The iridium layer on top is in a cube on cube orientation relationship to the YSZ, i.e., it shows the identical rotation with respect to the Si substrate (for further details, see Sec. III C). The mosaic spread of the iridium layers is 0.2° for the tilt and 0.28° for the twist. These values are only slightly higher than for heteroepitaxial layers on Si(001).<sup>14</sup> It is important to note that the oxide as well as the metal layer consist of one single texture component without any indication of twins.

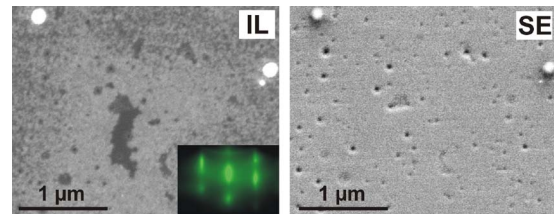


FIG. 1. (Color online) SEM micrographs of an Ir/YSZ/Si(111) sample after BEN acquired with two different secondary electron detectors (IL and SE detector). Sampled area and scale are identical in both images. The inset shows a RHEED pattern taken along the Ir[110] direction.

#### B. BEN on Ir/YSZ/Si(111)

In many former studies the successful nucleation of diamond on Ir(001) became manifest as bright areas when imaged in the SEM by the IL detector.<sup>12</sup> Imaging the same spot by the standard lateral secondary electron (SE) detector, the domains are nearly invisible. Figure 1 shows the surface of an Ir/YSZ/Si(111) sample after the BEN process imaged with the two detectors. Bright regions are visible in the IL detector image while the identical area yields no contrast in the SE image. This directly leads us to two important conclusions: first, domain formation is a general phenomenon on Ir(111), too, and second, diamond nucleation was successful on this sample.

The inset in Fig. 1 contains the RHEED pattern taken from the surface of the same sample after BEN. The structure of the pattern, a transition from streaky to spotlike, is attributed to a weak roughening of the iridium surface. No traces of diamond related spots are visible. Both observations are in accordance with the former results for BEN on Ir(001) surfaces.<sup>15,16</sup>

Figure 2(a) shows a cross section TEM micrograph of a BEN sample after successful nucleation as deduced from the SEM images. An additional 6-nm-thick Ir layer was evaporated on top of the sample to protect it during TEM sample preparation and to facilitate the imaging of the thin BEN layer. The bright slit with an average thickness of 1.3 nm between the iridium substrate film and the Ir covering layer can be attributed to the carbon film deposited by BEN. In high resolution images taken at several different positions along the slit, no indications of crystalline diamond nuclei

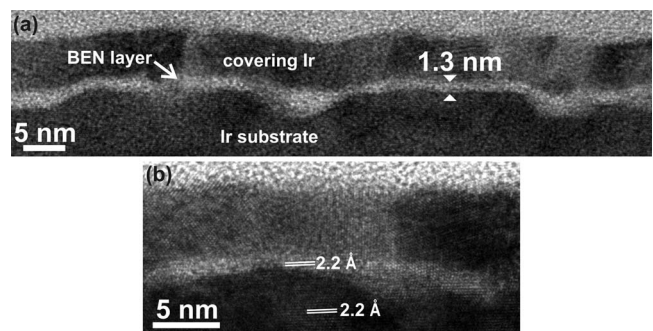


FIG. 2. Cross section TEM images of a BEN layer on Ir/YSZ/Si(111) (Ir[110] zone axis). Before TEM sample preparation the BEN layer was covered by additional 6 nm Ir. In (a) the thickness of the BEN layer is shown, while the atomic resolution in (b) allows to evaluate the spacing between the {111} planes visible in the Ir substrate and in the BEN layer.

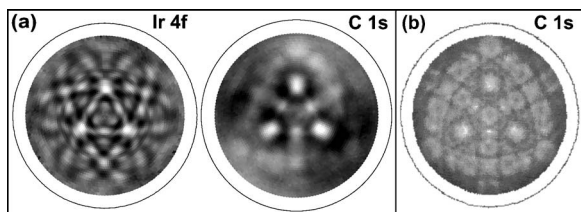


FIG. 3. XPD patterns of (a) the Ir  $4f_{7/2}$  and C  $1s$  core levels for the Ir/YSZ/Si(111) sample after BEN. (b) C  $1s$  XPD pattern of diamond (111) single crystal surface taken from Ref. 17. The C  $1s$  pattern of the BEN layer contains the raw data without any symmetry averaging (i.e., without three-fold averaging). The scale bar is 0.9 for black and 1.2 for white. The maximum anisotropy in the C  $1s$  pattern of the BEN layer, as defined in Refs. 15 and 18, amounts to 32% (measured at a polar angle of  $32^\circ$ ).

could be found. Atomically resolved structures within the BEN layer [see Fig. 2(b)], which are sometimes observed, correspond to Ir and cannot be attributed to diamond.

X-ray photoelectron spectroscopy (XPS) is an additional method that was applied to obtain an independent quantification of the carbon coverage on the iridium. Assuming a homogeneous, closed carbon layer a thickness of 6 monolayers (MLs) was determined with 1 ML diamond (111) equals 0.206 nm. This value fits well the width of the slit seen in the cross section TEM images.

An XPD pattern of the Ir  $4f_{7/2}$  photoelectrons is presented in Fig. 3(a). The pattern exhibits a threefold symmetry as expected for the Ir(111) surface. There are no differences between the diffractograms of an as-grown Ir film (not shown here) and of an Ir(111) surface after BEN.

XPD measurements were also taken for the C  $1s$  photoelectrons. They yield a distinct pattern with a high contrast that exhibits a clear threefold symmetry [see Fig. 3(a)]. For comparison, the diffractogram of a single crystal taken from Ref. 17 is included in Fig. 3(b). The main intensity maxima and the dominant bands are nearly identical in both patterns. This indicates that a high fraction of the carbon atoms at the surface of the sample is arranged in a crystalline diamond structure. The single crystal measurement, however, shows significantly more fine structures.

### C. Characterization of the diamond layers on Ir/YSZ/Si(111) after few hours of growth

After the successful BEN treatment, several samples have been grown for 3 h in a standard CVD diamond pro-

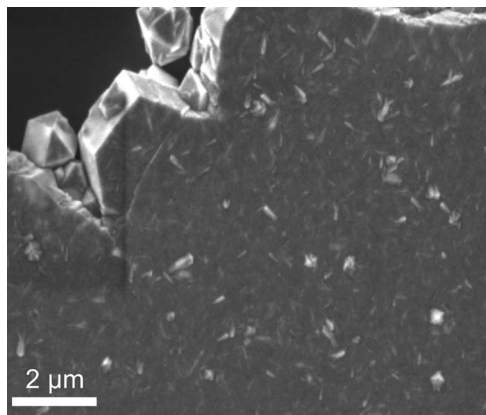


FIG. 4. SEM micrograph of a  $1.5 \mu\text{m}$  thick diamond film on Ir/YSZ/Si(111).

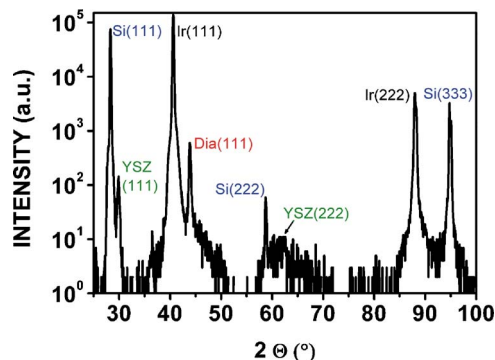


FIG. 5. (Color online)  $\Theta-2\Theta$  scan of a  $1.5 \mu\text{m}$  thick diamond film on Ir/YSZ/Si(111).

cess. The surface of one of these diamond films is shown in Fig. 4. The image was taken at the edge of the film in order to highlight the side facets of the grains.

Figure 5 shows a  $\Theta-2\Theta$  scan of one of these films with a thickness of about  $1.5 \mu\text{m}$ . All peaks can be assigned to silicon, YSZ, iridium, and diamond reflections of the type (111) or the corresponding higher order peaks. The weak signal at  $2\Theta=58.84^\circ$  stems from the forbidden Si(222) reflection. There is no indication of alternative phases or other texture components including polycrystalline material.

The epitaxial alignment of the sample was deduced from XRD pole figures. In Fig. 6 the three Si{111} peaks besides the central one define the orientation of the silicon substrate. The YSZ layer on top of the silicon shows the same symmetry but rotated by  $60^\circ$  about the surface normal. No additional peaks, e.g., due to twins, are visible. The maxima in the iridium and diamond pole figures are identical to those of YSZ, i.e., they are all rotated by  $60^\circ$  with respect to the Si substrate lattice. The epitaxial relationship of the stack is  $\text{Dia}(111)[1\bar{1}0] \parallel \text{Ir}(111)[1\bar{1}0] \parallel \text{YSZ}(111)[1\bar{1}0] \parallel \text{Si}(111)[0\bar{1}1]$ .

The diamond pole figure is clearly dominated by the epitaxial peaks. In order to check for additional peaks due to grains in twin position we made a further azimuthal scan of

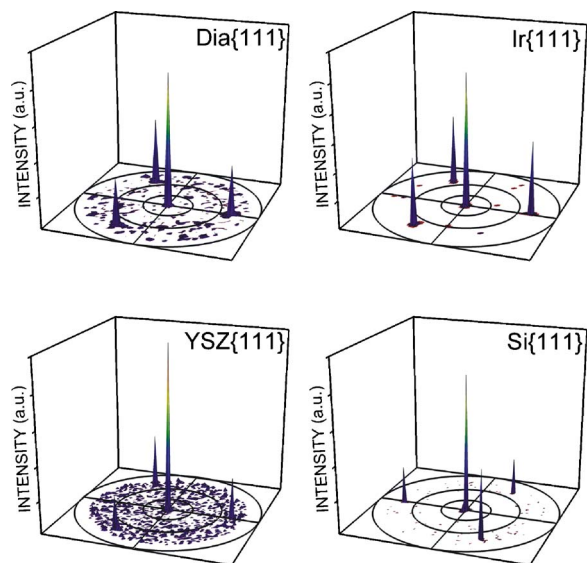


FIG. 6. (Color online) XRD pole figures of Si, YSZ, Ir, and diamond reflections measured on the sample shown in Fig. 4.

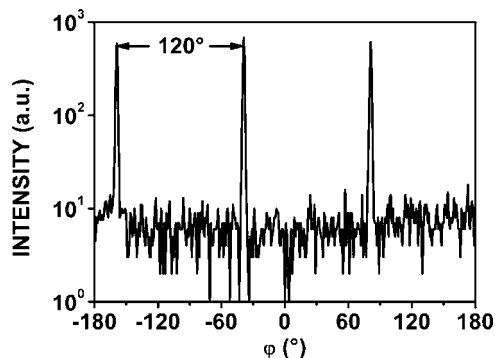


FIG. 7.  $\varphi$  scan for the diamond  $\{111\}$  reflections measured at a polar angle  $\chi=70.53^\circ$ . Contact twins would yield peaks shifted by  $60^\circ$  relative to the maxima of the epitaxial grains.

the diamond  $\{111\}$  reflection ( $2\Theta=43.92^\circ$ ) at  $\chi=70.5^\circ$  with higher angular resolution. In this scan, contact twins on a (111) surface should appear as additional peaks midway between the maxima of the epitaxial grains. From the intensity profile in Fig. 7 we estimate the twinning ratio to be lower than 1%.

Finally, the mosaic spread of this film has been determined by high resolution rocking curves and azimuthal scans of the diamond  $\{111\}$  reflections. The full width at half maximum for the tilt and twist angular distribution is  $0.96^\circ$  and  $1.85^\circ$ , respectively.

#### IV. DISCUSSION

In the present work we have shown that epitaxial diamond nucleation by BEN is also possible on Ir(111). Many of the features formerly observed on Ir(001) are also present on this surface. First of all the domains marking the location of the diamond nuclei are clearly visible. In spite of this unequivocal proof of successful nucleation, we could not find any indication of crystalline diamond in RHEED and cross section HRTEM.

The thickness of the carbon nucleation layer of 1.2–1.3 nm, as deduced from HRTEM and XPS, is in the range of values found on Ir(001).<sup>15,16,18–21</sup> In contrast to RHEED and TEM, XPD yields clear patterns that resemble reference measurements on (111) single crystal diamond surfaces except for less fine structure in the pattern of the BEN layer. The most intriguing feature of the XPD results consists of the threefold symmetry which means that the diamond nuclei grow in a perfect epitaxial orientation relationship. Even the strong ion bombardment did apparently not induce defects generating diamond in twin orientation relationship. As discussed for BEN on Ir(001), the ion bombardment induced defects may be responsible for the disappearance of some fine structure. All the present observations concerning the BEN layer allow the conclusion that the mechanisms of diamond nucleation on Ir(111) are absolutely identical to those on Ir(001).

The samples that have been grown for 3 h exhibit pole figures typical for epitaxial diamond without any additional texture components. This is rather surprising since twinning is a critical issue for growth on (111) surfaces. Two different classes of twins can be distinguished. Common to all is the

crystallographic type of twin plane which is  $\{111\}$ . For the penetration twins with three different orientations this plane is inclined by  $70.5^\circ$  relative to the (111) substrate surface. In contrast, the contact twins share the twin plane parallel to the substrate surface with the epitaxial matrix. The overgrowth of twins by choosing dedicated process conditions should only work for penetration twins.<sup>9</sup>

Over many years Tachibana *et al.*<sup>22</sup> studied epitaxial diamond growth on Pt(111). They always found a huge fraction of diamond grains in contact twin orientation. The intensity ratio of the two variants, i.e., epitaxial grains and contact twins, varied from about 20% to more than 60% with increasing thickness.<sup>22</sup> They attributed it to double positioning at the heterointerface and twin formation during the subsequent growth.<sup>23</sup> Suppressing the twins by use of off-axis substrates was tested but turned out not to be very efficient.<sup>24</sup> In our former work on Si(111), twinning was also very strong.<sup>25</sup> Compared with these earlier results, the films on Ir(111) presented in this study behave in a completely different way. Neither in the nucleation stage nor during the growth stage any significant twinning had occurred.

The mosaic spread of  $0.96^\circ$  (tilt) and  $1.85^\circ$  (twist) has to be compared with the few values reported on alternative systems. On Si(111) we obtained a tilt value of  $8^\circ$ .<sup>26</sup> On Pt(111) the mosaicity was typically in the range of several degrees. We found only one publication in which a rocking curve width of  $1.1^\circ$  was reported for growth on a Pt(111)/Ir(111)/Pt(111)/Al<sub>2</sub>O<sub>3</sub>(0001) substrate.<sup>27</sup> The absence of any information on the twist value in this paper does not allow an adequate comparison with the present result, which is the first report on heteroepitaxial diamond films with a tilt below  $1^\circ$ .

#### V. SUMMARY AND CONCLUSIONS

The present work describes the first systematic study on successful diamond nucleation on Ir(111) using the BEN technique in a MWPCVD setup. Heteroepitaxial multilayer samples with the structure Ir/YSZ/Si(111) were prepared as new substrates for diamond nucleation on Ir(111). The mosaic spread of the Ir films was  $0.2^\circ$  (tilt) and  $0.28^\circ$  (twist). All the typical phenomena reported for BEN on Ir(001) were also found on Ir(111). The gathering of the diamond nuclei in domains, unique for diamond nucleation on iridium, has now been shown for the (111) surface, too. The carbon layer thickness in the range of 1–2 nm and the absence of crystalline diamond structures in RHEED and HRTEM are identical to BEN on Ir(001). In XPD, C 1s patterns with high contrast were measured. The main features are comparable with measurements on diamond (111) single crystal surfaces. The weaker fine structure is attributed to some disorder due to the ion bombardment. The clear threefold symmetry, however, indicates that this ion bombardment did not induce any measurable amount of twinning. Even after 3 h growth of an epitaxial diamond layer, twinning is still negligible, i.e., below 1%. The epitaxial relationship of the stack is  $\text{Dia}(111)[1\bar{1}0]\parallel\text{Ir}(111)[1\bar{1}0]\parallel\text{YSZ}(111)[1\bar{1}0]\parallel\text{Si}(111)[0\bar{1}1]$ . With a mosaic spread of  $0.96^\circ$  (tilt) and  $1.85^\circ$  (twist) these diamond films represent the best heteroepitaxial films with

(111) orientation reported up to now. They provide interesting growth substrates, e.g., for phosphorous doped diamond.

The formation of UV-light emitting heterostructure diodes by depositing (0001)-oriented AlN on (001)-oriented *p*-doped diamond has recently been demonstrated.<sup>28,29</sup> Due to the different symmetry [sixfold for AlN(0001) and fourfold for diamond(001)] different variants appear that prevent the formation of a single crystal film. On diamond(111), AlN with one single texture component can be expected. Since the preparation of Ir/YSZ/Si wafers with a size of 4 in. has recently been demonstrated,<sup>30</sup> the future preparation of heterojunction devices using (0001) oriented wurtzite-type wide band gap semiconductor layers (such as AlN, GaN, and ZnO) on diamond/Ir/YSZ/Si(111) substrates now appears as a technologically attractive and feasible option.

We gratefully acknowledge the financial support of this work from the European community within the training network DRIVE (Grant No. MRTN-CT-2004-512224 for R.B.) and the STREP project NANOMESH (Grant No. NMP4-CT-2004-013817 for S.G.).

- <sup>1</sup>K. Ohtsuka, K. Suzuki, A. Sawabe, and T. Inuzuka, *Jpn. J. Appl. Phys., Part 2* **35**, L1072 (1996).
- <sup>2</sup>M. Schreck, H. Roll, and B. Stritzker, *Appl. Phys. Lett.* **74**, 650 (1999).
- <sup>3</sup>C. Bednarski, Z. Dai, A.-P. Li, and B. Golding, *Diamond Relat. Mater.* **12**, 241 (2003).
- <sup>4</sup>M. Schreck, F. Hörmann, H. Roll, J. K. N. Lindner, and B. Stritzker, *Appl. Phys. Lett.* **78**, 192 (2001).
- <sup>5</sup>K. Ohtsuka, H. Fukuda, K. Suzuki, and A. Sawabe, *Jpn. J. Appl. Phys., Part 2* **36**, L1214 (1997).
- <sup>6</sup>Z. Dai, C. Bednarski-Meinke, R. Loloee, and B. Golding, *Appl. Phys. Lett.* **82**, 3847 (2003).
- <sup>7</sup>T. Bauer, S. Gsell, M. Schreck, J. Goldfuß, J. Lettieri, D. G. Schlom, and B. Stritzker, *Diamond Relat. Mater.* **14**, 314 (2005).
- <sup>8</sup>S. Gsell, T. Bauer, J. Goldfuß, M. Schreck, and B. Stritzker, *Appl. Phys. Lett.* **84**, 4541 (2004).
- <sup>9</sup>C. Wild, R. Kohl, N. Herres, W. Müller-Sebert, and P. Koidl, *Diamond Relat. Mater.* **3**, 373 (1994).
- <sup>10</sup>S. Koizumi, M. Kamo, Y. Sato, H. Ozaki, and T. Inuzuka, *Appl. Phys.*

- Lett.* **71**, 1065 (1997).
- <sup>11</sup>S. Koizumi, K. Watanabe, F. Hasegawa, and H. Kanda, *Science* **292**, 1899 (2001).
- <sup>12</sup>M. Schreck, Th. Bauer, S. Gsell, F. Hörmann, H. Bielefeldt, and B. Stritzker, *Diamond Relat. Mater.* **12**, 262 (2003).
- <sup>13</sup>T. Greber, O. Raetz, T. J. Kreuz, P. Schwaller, W. Deichmann, E. Wetli, and J. Osterwalder, *Rev. Sci. Instrum.* **68**, 4549 (1997).
- <sup>14</sup>S. Gsell, M. Fischer, R. Brescia, M. Schreck, P. Huber, F. Bayer, B. Stritzker, and D. G. Schlom, *Appl. Phys. Lett.* **91**, 061501 (2007).
- <sup>15</sup>S. Gsell, S. Berner, T. Brugger, M. Schreck, R. Brescia, M. Fischer, T. Greber, J. Osterwalder, and B. Stritzker, *Diamond Relat. Mater.* **17**, 1029 (2008).
- <sup>16</sup>R. Brescia, M. Schreck, S. Gsell, M. Fischer, and B. Stritzker, *Diamond Relat. Mater.* **17**, 1045 (2008).
- <sup>17</sup>O. M. Küttel, R. G. Agostino, R. Fasel, J. Osterwalder, and L. Schlappbach, *Surf. Sci.* **312**, 131 (1994).
- <sup>18</sup>S. Kono, T. Takano, T. Goto, Y. Ikejima, M. Shiraishi, T. Abukawa, T. Yamada, and A. Sawabe, *Diamond Relat. Mater.* **13**, 2081 (2004).
- <sup>19</sup>Th. Bauer, M. Schreck, F. Hörmann, A. Bergmaier, G. Dollinger, and B. Stritzker, *Diamond Relat. Mater.* **11**, 493 (2002).
- <sup>20</sup>M. Schreck, F. Hörmann, S. Gsell, Th. Bauer, and B. Stritzker, *Diamond Relat. Mater.* **15**, 460 (2006).
- <sup>21</sup>S. Kono, M. Shiraishi, N. I. Plusnin, T. Goto, Y. Ikejima, T. Abukawa, M. Shimomura, Z. Dai, C. Bednarski-Meinke, and B. Golding, *New Diamond Front. Carbon Technol.* **15**, 363 (2005).
- <sup>22</sup>T. Tachibana, Y. Yokota, K. Kobashi, and Y. Shintani, *J. Appl. Phys.* **82**, 4327 (1997).
- <sup>23</sup>T. Tachibana, Y. Yokota, K. Miyata, T. Takashi, K. Kobashi, M. Tarutani, Y. Takai, R. Shimizu, and Y. Shintani, *Phys. Rev. B* **56**, 15967 (1997).
- <sup>24</sup>T. Tachibana, Y. Yokota, K. Hayashi, K. Miyata, and K. Kobashi, *Proceedings of the ADC/FCT'99*, edited by M. Yoshikawa, Y. Koga, Y. Tzeng, C.-P. Klages, and K. Miyoshi, Tsukuba, Japan, 31 August–3 September 1999 (unpublished), pp. 79–82.
- <sup>25</sup>K. Helming, S. Geier, M. Schreck, R. Heßmer, B. Stritzker, and B. Rauschenbach, *J. Appl. Phys.* **77**, 4765 (1995).
- <sup>26</sup>M. Schreck, R. Heßmer, S. Geier, B. Rauschenbach, and B. Stritzker, *Diamond Relat. Mater.* **3**, 510 (1994).
- <sup>27</sup>T. Tachibana, Y. Yokota, K. Hayashi, and K. Kobashi, *Diamond Relat. Mater.* **10**, 1633 (2001).
- <sup>28</sup>C. R. Miskys, J. A. Garrido, C. E. Nebel, M. Hermann, O. Ambacher, M. Eickhoff, and M. Stutzmann, *Appl. Phys. Lett.* **82**, 290 (2003).
- <sup>29</sup>C. R. Miskys, J. A. Garrido, M. Hermann, M. Eickhoff, C. E. Nebel, M. Stutzmann, and G. Vogg, *Appl. Phys. Lett.* **85**, 3699 (2004).
- <sup>30</sup>M. Fischer, S. Gsell, M. Schreck, R. Brescia, and B. Stritzker, *Diamond Relat. Mater.* **17**, 1035 (2008).